Phonon density of states of self-assembled isolated Fe-rich Fe-Pt alloy nanoclusters

B. Roldan Cuenya,[1,2,*] Jason R. Croy,[1] L. K. Ono,[1] A. Naitabdi,[1] H. Heinrich,[1,3] W. Keune,[4,5] J. Zhao,[6] W. Sturhahn,[6] E. E. Alp,[6] and M. Hu[6]

[1]*Department of Physics, University of Central Florida, Orlando, Florida 32816, USA*

[2]*Nanoscience Technology Center, University of Central Florida, Orlando, Florida 32816, USA*

[3]*Advanced Materials Processing and Analysis Center, University of Central Florida, Orlando, Florida 32816, USA*

[4]*Fachbereich Physik, Universität Duisburg–Essen, D-47048 Duisburg, Germany*

[5]*Max-Planck-Institut für Mikrostrukturphysik, D-06120 Halle, Germany*

[6]*Advanced Photon Source, Argonne National Laboratory, Argonne, Illinois 60439, USA*

(Received 10 June 2009; published 16 September 2009)

The Fe-projected phonon density of states (PDOS) of monolayer-thick films of self-assembled, size-selected, isolated $^{57}Fe_{1-x}Pt_x$ alloy nanoclusters (NCs) (height: ~2 nm, diameter: ~8 nm) supported on flat SiO_2/Si(111) substrates has been measured by nuclear resonant inelastic x-ray scattering. The samples were characterized by atomic force microscopy (AFM), transmission electron microscopy, and x-ray photoelectron spectroscopy (XPS). Surface segregation of Pt and PtSi formation at the NC surface due to the sample-preparation process is inferred from the XPS data. As compared to the bulk, pronounced modifications of the PDOS beyond the bulk cut-off energy are observed in bcc $^{57}Fe_{0.8}Pt_{0.2}$ (core)/PtSi(shell) NCs. By contrast, the PDOS of fcc $^{57}Fe_{0.75}Pt_{0.25}$ (core)/PtSi(shell) NCs retains features of bulk ordered Fe_3Pt Invar alloys (presumably due to a thicker PtSi shell), in particular, the transverse-acoustic [110] TA_1 mode near 9 meV. Apparently, this mode is not affected by size effects. The existence of the [110] TA_1 phonon mode is a prerequisite for the persistence of Invar-related effects in Fe_3Pt NCs. Important thermodynamic properties of the NCs are derived, such as the vibrational entropy per atom.

DOI: 10.1103/PhysRevB.80.125412 PACS number(s): 63.22.Kn, 63.20.D−, 65.80.+n

I. INTRODUCTION

The phonon density of states (PDOS), $g(E)$, describes the vibrational dynamics of atoms in solids and is a fundamental property that affects phase stability and phase transitions in alloys.[1,2] An important type of phase transition is the diffusionless (displacive) austenite (fcc)-to-martensite (bct) (or reverse) transformation in Fe-based Invar alloys, e.g., in $Fe_{65}Ni_{35}$ or Fe_3Pt alloys.[3,4] Invar alloys are ferromagnetic and of basic and technological significance owing to their remarkable properties, such as giant magnetovolume effect and small thermal expansion.[3,4] An important characteristic of Invar alloys, e.g., of $L1_2$-(Cu_3Au) ordered Fe_3Pt, is the pronounced softening of the low-energy (low-E) transverse-acoustic [110] TA_1 phonon mode (shear mode) upon cooling below the Curie temperature,[5–11] leading to elastic anomalies and martensitic transformation at low temperature.[3] These effects have been discussed in terms of enhanced electron-phonon interactions[5,6] due to the high electronic DOS of d electrons near the Fermi energy in Invar alloys.[12–14] Thus, detailed knowledge of the phonon spectrum is essential for the understanding of Invar-related properties.[15] Recently, Fe_3Pt nanowire arrays (with Invar composition) have been fabricated.[16,17] The fundamental question arises whether the Invar effect and the related martensitic transition are suppressed in Fe_3Pt (or other Invar-type) nanostructures due to finite-size effects. In Fe-Ni nanoclusters (NCs), the martensitic transition has been investigated experimentally[18] and the absence of structural instability below a certain NC size has been observed. According to theory[19,20] the transformation temperature upon heating scales with, and is inversely proportional to, NC diameter. This is contrary to the transformation upon cooling, which appears to be suppressed due to the high metastability of the fcc phase and the lack of nucleation sites. Recent molecular dynamics simulations for elemental Fe nanowires predict that the martensitic transition temperature is inversely proportional to the wire diameter during heating and depends linearly on applied axial tensile stress.[21] An essential prerequisite for the occurrence of the martensitic transformation in Invar alloy NCs is the existence of the [110] TA_1 phonon mode, since softening of this mode is the origin of this instability in the bulk.[3,5–8,15] Therefore, a fundamental question is whether the [110] TA_1 mode still exists in Invar-alloy NCs. This is not clear, since in isolated metallic NCs, due to their large surface-to-volume ratio, distinct modifications of the phonon spectrum as compared to the bulk PDOS have been predicted in Refs. 22–28 and recently observed on isolated supported Fe NCs.[28] Therefore, the experimental determination of the PDOS in Invar NCs is of fundamental importance.

This work presents an experimental study of the partial PDOS of isolated, monodispersed, bimetallic nanoclusters. Fe-projected PDOS curves, $g(E)$, were obtained from ^{57}Fe nuclear resonant inelastic x-ray scattering (NRIXS). As compared to the bulk case, we observe strong modifications of $g(E)$ of bcc $^{57}Fe_{0.8}Pt_{0.2}$ alloy NCs extending beyond the bulk cut-off energy. By contrast, such modifications are not found in fcc $^{57}Fe_{0.75}Pt_{0.25}$ alloy NCs with Invar composition. Here, characteristic features of the PDOS of bulk $L1_2$-ordered Invar (Fe_3Pt) alloys appear in $g(E)$ of the Invar alloy NCs, including a shoulder near ~9 meV which can be attributed to the [110] TA_1 mode of the Fe_3Pt Invar alloy. The existence of this phonon mode is a necessary condition for the persistence of Invar-related effects in low-dimensional systems.

Moreover, important thermodynamic properties of the NCs have been derived from the PDOS.

II. EXPERIMENTAL DETAILS AND SAMPLE CHARACTERIZATION

Monolayer-thick films of size-selected, isolated $^{57}Fe_{1-x}Pt_x$ NCs uniformly spaced over large surface areas were prepared by micelle encapsulation[28–31] of $^{57}FeCl_3$ and H_2PtCl_6 salts in PS(27700)-P2VP(4300) diblock copolymers. Samples of bimetallic clusters with two different nominal compositions of $^{57}Fe_{0.8}Pt_{0.2}$ (sample 1) and $^{57}Fe_{0.3}Pt_{0.7}$ (sample 2) were obtained by tuning the relative concentration ratio of the two metal salts.

NRIXS on the SiO_2/Si(111) supported ^{57}Fe-Pt NCs was performed at RT in air at beamlines 3-ID and HP-CAT16 of the Advanced Photon Source (Argonne) by tuning the synchrotron beam energy around the resonant energy of 14.4125 keV of the ^{57}Fe nucleus with an energy resolution of 2.3 meV (1.0 meV) for sample 1 (sample 2). The NRIXS method and the data evaluation for extracting $g(E)$ are described in detail elsewhere.[32–36]

Figure 1 shows atomic force microscopy (AFM) images from (a) sample 1 (nominal $^{57}Fe_{0.8}Pt_{0.2}$) and (b) sample 2 (nominal $^{57}Fe_{0.3}Pt_{0.7}$) containing NCs deposited on SiO_2/Si(111). The average NC height before Ar^+ etching for these samples is 2.1 ± 0.4 nm. The etching did not result in distortions of the NC's spatial arrangement. It did, however, provide an ultrathin Si coating due to sputtering of Si atoms from the Si(111) substrate that prevented the NCs from oxidation upon air exposure, as evidenced by our cross-sectional transmission electron microscopy (TEM) [Fig. 1(c)] and x-ray photoelectron spectroscopy (XPS) data (see below).

High-resolution-TEM (HR-TEM) images from samples 1 and 2 (NCs deposited on C-coated Cu grids) are shown in Figs. 1(d) and 1(e), respectively. Single-grain NCs were observed in the case of sample 1, while multifaceted grains were detected in sample 2. The resolution of our TEM was not sufficient to detect a shell around the NC core. From these images, the typical cluster diameters are ~8.2 nm. According to our TEM and AFM data the aspect ratio (diameter/height) of our NCs is ~4. From the fast Fourier transform analysis of the TEM images in Figs. 1(d) and 1(e), a lattice parameter of $a=0.309 \pm 0.007$ nm (0.379 ± 0.007 nm) was determined for sample 1 (sample 2), assuming the bcc (fcc) phase. Our NRIXS results (see below) support the bcc (fcc) structure for sample 1 (sample 2). As a reference, the lattice parameters of bulk alloys with composition $Fe_{0.8}Pt_{0.2}$ (bcc) and $Fe_{0.75}Pt_{0.25}$ (fcc, Fe_3Pt) are given by 0.297 nm (extrapolated from data in Ref. 37) and 0.375 nm,[38] respectively. Comparison indicates that the NCs in sample 1 are close to bcc $Fe_{0.8}Pt_{0.2}$, i.e., close to the nominal composition, while the NCs in sample 2 are close to fcc $Fe_{0.75}Pt_{0.25}$, which differs significantly from the nominal cluster composition of $Fe_{0.3}Pt_{0.7}$. As will be discussed later, this is attributed to the segregation of Pt to the NC surface leaving an Fe-rich core.

Figure 2 displays XPS spectra from the (a) Fe $2p$ and (b) Pt $4f$ core-level regions of NCs, in sample 2 [(i) and (ii)] and sample 1 [(iii) and (iv)], deposited on SiO_2/Si(111). Ar^+ etching resulted in an ultrathin Si coating on the samples that largely protected the NCs against oxidation, since no Fe^{3+} signal (e.g., Fe^{3+} $2p_{3/2}$ in Fe_2O_3: at 711 eV)[39] was detected on these samples by XPS after air exposure. The binding energy (BE) of Fe in these bimetallic clusters ($2p_{3/2}$, 707.3 eV) is in agreement with that of metallic iron (707.0–707.3 eV)[39] or $Fe_{0.48}Pt_{0.52}$ films (707.5 eV).[40] By contrast, a very large BE was measured for Pt in our NC samples ($4f_{7/2}$, 73.0–73.1 eV) before and after air exposure. These BEs are up to +2.0 eV larger than for bulk Pt^0 ($4f_{7/2}$, 71.1 eV)[39] and are attributed to the formation of PtSi ($4f_{7/2}$, 73 eV).[41] Our annealing treatment in vacuum (at 500 °C) resulted in preferential segregation of Pt to the NC surface, which readily reacted with Si during the subsequent Ar^+-etching procedure. This trend for Pt segregation is in agreement with calculations and experimental results on Fe-Pt systems.[42–44] We infer that our NCs carry a thin PtSi shell, which is much thinner for the NCs in sample 1 because of its weaker Pt-$4f$ signal (20% Pt content) as compared to sample 2 (70% Pt content), and because the nominal and actual compositions of the NC core ($Fe_{0.8}Pt_{0.2}$) agree fairly well with each other, contrary to the case of sample 2. We expect that the observed

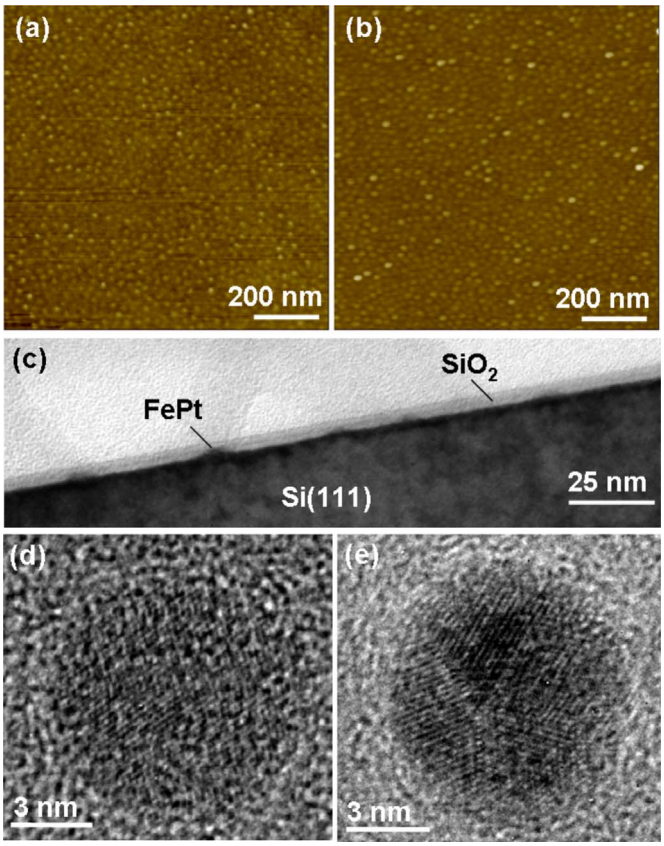

FIG. 1. (Color online) AFM and HR-TEM images of sample 1 [(a) and (d)] and sample 2 [(b) and (e)], with Fe-Pt alloy NCs synthesized as described in the text. (c) Cross-sectional TEM image of nanoclusters similar to those in sample 2, but synthesized using PS(81000)-PVP(14200) and deposited on SiO_2/Si(111). All images were taken after polymer removal by annealing in UHV at 500 °C and subsequent Ar^+-sputter etching (0.5 keV, 20 min) at room temperature.

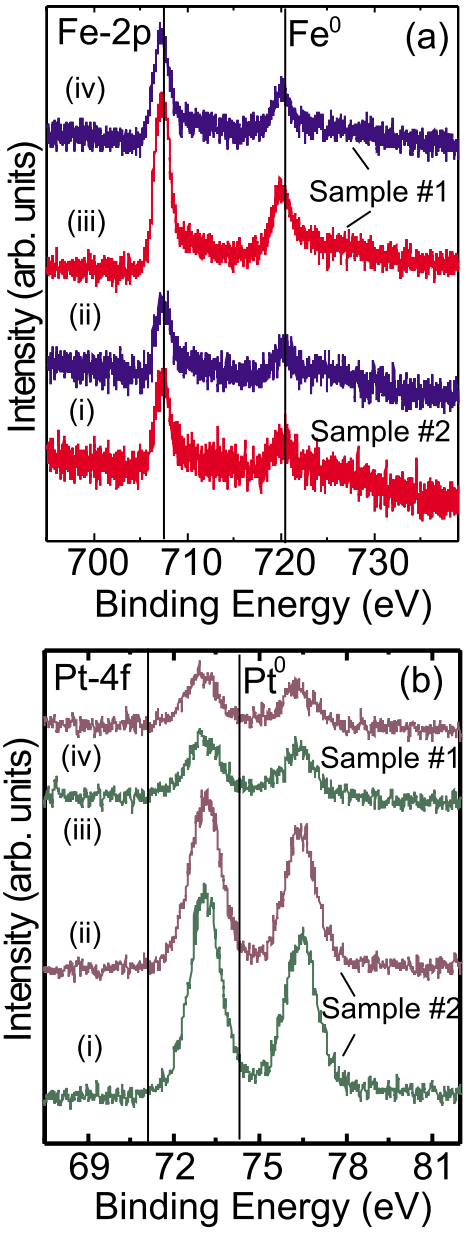

FIG. 2. (Color online) XPS spectra (Al $K\alpha$=1486.6 eV) of the (a) Fe-2p and (b) Pt-4f core levels of similarly sized Fe-Pt alloy nanoclusters in samples 1 and 2 deposited on SiO_2/Si(111). The spectra were measured after polymer removal by annealing in UHV at 500 °C followed by Ar^+-sputter-etch [(i) and (iii)], and after subsequent air exposure for 4 days [(ii) and (iv)].

Pt surface segregation and PtSi shell formation will influence the PDOS of the NCs (see below).

III. NRIXS RESULTS AND DISCUSSION

Figure 3 displays NRIXS spectra (raw data) of (a) sample 1 (NC core: bcc $^{57}Fe_{0.8}Pt_{0.2}$) and (b) sample 2 (NC core: fcc $^{57}Fe_{0.75}Pt_{0.25}$). The main features of these spectra are an intense elastic peak at E=0 meV (Mössbauer or zero-phonon line) and side bands at higher and lower excitation energies E corresponding to phonon-assisted excitation of the nuclear

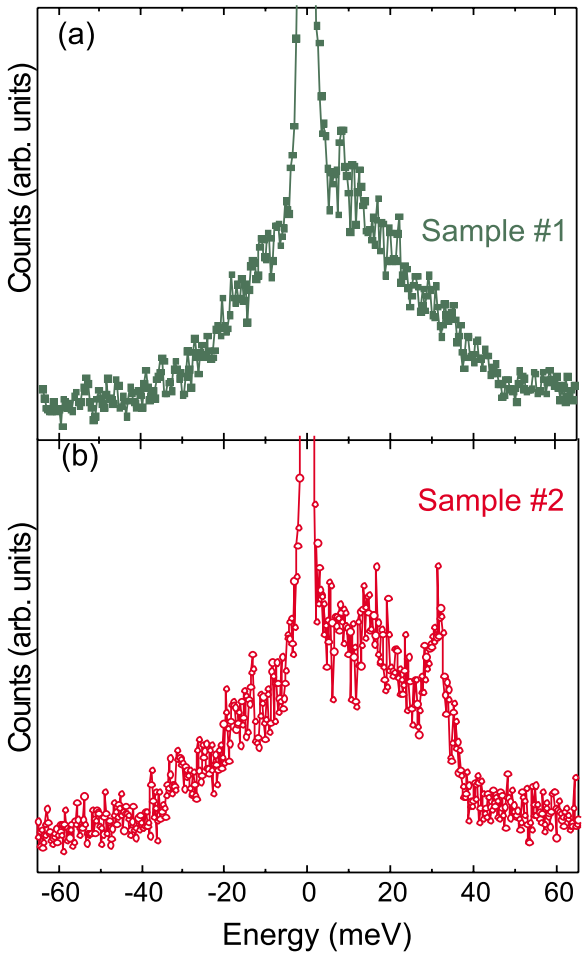

FIG. 3. (Color online) Experimental NRIXS spectra (raw data) taken at RT from Fe-Pt alloy NCs supported on SiO_2/Si(111): (a) sample 1 (bcc alloy) and (b) sample 2 (fcc alloy).

resonance by photons via phonon creation ($E>0$) and annihilation ($E<0$). A broad and nearly structureless phonon excitation spectrum is observed for sample 1 [Fig. 3(a)], while sharper phonon features near ~31 and ~13 meV and a cut-off near 40 meV are noticed for sample 2, Fig. 3(b).

Figure 4(a) presents the Fe-projected (partial) PDOS, $g(E)$, of sample 1 (bcc $^{57}Fe_{0.8}Pt_{0.2}$) (full squares) and of a reference bulk bcc ^{57}Fe foil (full-drawn line), obtained from measured data. Also shown is the PDOS of a reference NC sample (reproduced from Ref. 28, full circles) containing similarly sized, isolated, elemental bcc ^{57}Fe NCs (of ~2.3 nm average AFM height), subjected to an identical preparation technique and carrying an Fe-oxide shell,[28] sample 3. Clear differences between $g(E)$ of sample 1 and bulk bcc Fe are observed: (i) the strong suppression of the longitudinal acoustic (LA) phonon peak at ~36 meV and of the transverse acoustic (TA) modes near ~27 and ~22 meV, an effect that may be attributed to phonon damping due to confinement.[45,46] However, a residue of the 36 meV phonon peak is visible in the $g(E)$ of sample 1, which proves the existence of the bcc structure in the $^{57}Fe_{0.8}Pt_{0.2}$ NCs, in agreement with our TEM results. (ii) The enhancement of $g(E)$ at low and high energies, where excitations extend beyond the cut-off energy of ~40 meV of bulk bcc

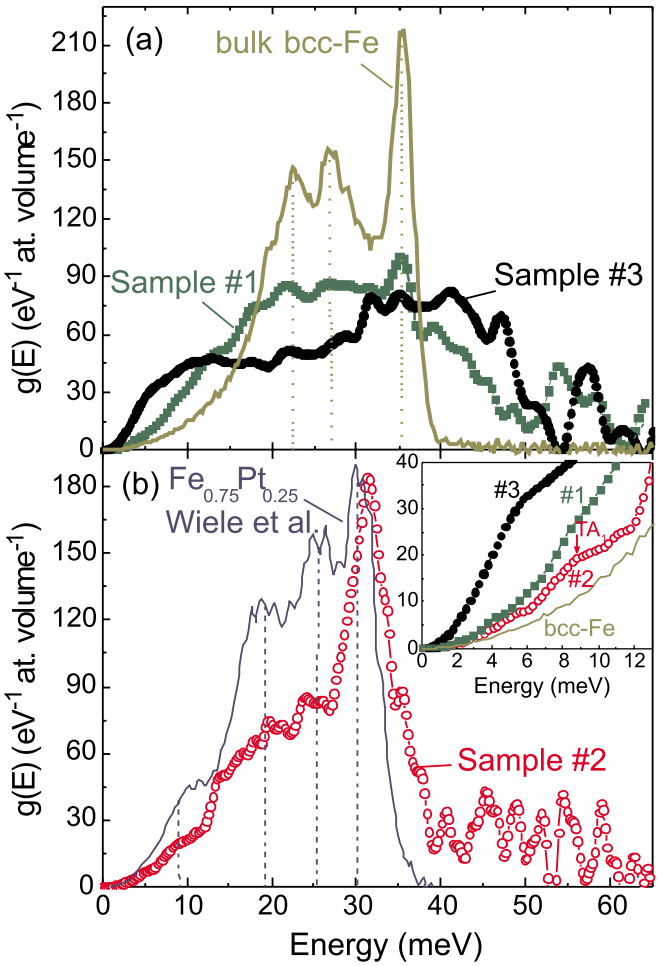

FIG. 4. (Color online) PDOS, $g(E)$, of Fe-Pt NCs, obtained from the data in Fig. 3: (a) sample 1 (bcc $^{57}Fe_{0.8}Pt_{0.2}$) (full squares). Also shown: measured $g(E)$ of bulk bcc ^{57}Fe (full-drawn curve) and of elemental bcc ^{57}Fe NCs (sample 3) from Ref. 28 (full circles). (b) sample 2 (fcc $^{57}Fe_{0.75}Pt_{0.25}$) (open circles). Also shown: measured $g(E)$ of a bulk $L1_2$-ordered $Fe_{0.75}Pt_{0.25}$ Invar alloy (Refs. 10 and 11) (full-drawn curve). Inset in (b): low-energy part of $g(E)$.

Fe. This effect is less pronounced than for sample 3.[28] According to theory, the low-E enhancement is attributed to low-coordinated vibrational surface states,[22–28] while the high-energy (high-E) enhancement has been predicted to depend on compressive stress due to enhanced capillary forces in the NCs[22,47] or to shrinkage of near-neighbor atomic bond lengths of specific atoms relative to bulk.[23–27] In fact, it was observed experimentally in isolated ^{57}Fe NCs that the low- and high-E enhancements in $g(E)$ depend on the thickness and type of the Fe-containing shell around the ^{57}Fe NCs [i.e., Fe_2O_3 or Fe_3C (Ref. 28)]. Therefore, the remarkable decrease in the low-E and high-E regions of the PDOS of sample 1, as compared to that of sample 3 [Fig. 4(a)], can be attributed to the different shell structures (PtSi versus $^{57}Fe_2O_3$). Since we measure the ^{57}Fe-projected PDOS, the presence of Pt and Si atoms (and the decrease in the number of ^{57}Fe atoms) at the NC surface of our sample 1 is expected to reduce the low-E part of $g(E)$ as compared to pure ^{57}Fe NCs.

The striking features of the Fe-projected PDOS of sample 2 (fcc $^{57}Fe_{0.75}Pt_{0.25}$) (open circles) are a strong and dominant peak at ~31 meV and relatively weak PDOS in the medium- and low-E regimes of $g(E)$, with weak bands near ~20 and ~25 meV, Fig. 4(b). The ~31 meV peak lies at significantly lower energy than the main 36 meV peak of bulk bcc Fe, Fig. 4(a). The cut-off energy of sample 2 is at ~40 meV, as is also revealed by the NRIXS raw data, Fig. 3(b).[48]

For comparison, we have reproduced in Fig. 4(b) (full-drawn line) the $g(E)$ curve of $L1_2$-ordered bulk $Fe_{0.75}Pt_{0.25}$ Invar alloy (with a long-range order parameter S=0.8) measured also by NRIXS by Wiele *et al.*[10,11] A comparison of these two $g(E)$ curves reveals distinct differences, but also similarities: (i) both $g(E)$ curves span roughly the same energy range; (ii) the strong PDOS peak at ~31 meV in sample 2 almost coincides with the most intense peak in $g(E)$ at ~30 meV (optical phonon modes[5,6]) in the bulk Invar sample; (iii) the weak peaks near ~20 and ~25 meV for sample 2 coincide with phonon bands (other optical phonons[5,6]) at analogous positions in the bulk Invar sample; however, these phonon bands are considerably reduced in their $g(E)$ intensity (by about 50%) in the NCs of sample 2 as compared to $g(E)$ of the bulk Invar alloy; (iv) a small blueshift of the cut-off energy from ~38 meV in the bulk Invar sample to ~40 meV in sample 2 exists; (v) a shoulder at ~9 meV is visible in the $g(E)$ of both samples, although $g(E)$ at the shoulder of sample 2 is reduced (by ~50%) relative to that of the bulk Invar sample [Fig. 4(b) and insert]. The energy of this shoulder (~9 meV) agrees well with that of the [110] TA_1 mode (at the Brillouin zone boundary) in bulk ordered Fe_3Pt at RT.[5–11] This can be seen in the inelastic neutron scattering (INS) results by Noda and Endoh.[6] In Fig. 1 (panel for Σ_4) of Ref. 6, the [110] TA_1 dispersion curve of bulk ordered Fe_3Pt Invar alloy at 295 K can be observed to merge horizontally at the zone boundary (at a reduced wave vector ζ[110]=0.5) at a phonon energy of ~9 meV. This implies zero group velocity and enhanced $g(E)$ at that energy. Similar features (and, moreover, the mode softening upon cooling) can be seen in the [110] TA_1 disperson curve of $L1_2$-ordered $Fe_{72}Pt_{28}$ Invar alloy, obtained by Kästner *et al.*[8] from INS (see Fig. 1 of Ref. 8). Wiele *et al.*[10] and Wiele,[11] in their NRIXS work, identified the shoulder near 9 meV in $g(E)$ of bulk ordered Fe-Pt Invar alloys with the [110] TA_1 mode and, in fact, observed a redshift (phonon softening) of this mode upon decreasing the temperature, in qualitative agreement with the INS results.[6,8] Therefore, by analogy with the literature reports just described, we attribute the $g(E)$ shoulder at ~9 meV, observed in our Fig. 4(b) for sample 2, to the [110] TA_1 phonon mode responsible for the soft-mode behavior in bulk Fe_3Pt Invar alloys and for the martensitic transition at low T.[3,7–11]

The appearance of the [110] TA_1 phonon mode in $g(E)$ of sample 2 unambiguously proves that Pt atoms are dissolved in the fcc Fe lattice of the core of these NCs, and that the average alloy composition in the core is on the Fe-rich side, in agreement with our TEM results. This follows from the fact that at the Brillouin zone boundary of the [110] TA_1 phonon mode only Fe atoms vibrate in a rigid cubic lattice of heavy Pt atoms [M_2 and M_4 modes in ordered Fe_3Pt (Refs.

TABLE I. Thermodynamic parameters derived from NRIXS measurements.

Sample	Lamb-Mössbauer factor	Kinetic energy (meV/atom)	Vibrational entropy (k_B/atom)	Vibrational specific heat (k_B/atom)
$Fe_{0.8}Pt_{0.2}$ NCs (bcc), sample 1	0.742 (4)	43.8 (6)	3.00 (6)	2.63 (8)
$Fe_{0.75}Pt_{0.25}$ NCs (fcc), sample 2	0.773 (4)	44.1 (8)	2.91 (6)	2.61 (9)
Fe NCs (bcc), sample 3 (Ref. 28)	0.612 (3)	45.0 (9)	2.95 (7)	2.6 (1)
Fe Nanocrystalline (Ref. 45)	0.755 (1)	43.2 (1)	3.17 (2)	2.68 (2)
Fe NCs (fcc) in Cu (Ref. 52)	0.734 (4)			
bcc Fe (bulk) (Ref. 53)	0.7951(6)	42.54(6)	3.133(9)	2.723(9)

5–8)]. Also important in this context is the observation by Fultz *et al.*[49] that on the Pt-rich alloy side, $L1_2$-ordered bulk $FePt_3$ alloys exhibit a dominant sharp peak (optical phonons) in $g(E)$ at 25 meV, i.e., at significantly lower energy than our ~31 meV peak, mainly caused by the higher average mass of $FePt_3$ as compared to Fe_3Pt. Further, no significant feature of the TA_1 mode near ~7–9 meV is observed in $g(E)$ of Pt-rich $L1_2$-ordered bulk $FePt_3$.[49] From these considerations and from observations (i)–(iii) and (v) above, we conclude that the core of the alloy NCs in our sample 2 is close to the Fe_3Pt Invar composition and is highly $L1_2$ ordered due to the relatively high annealing temperature of 500 °C under UHV conditions. Since the presence of the [110] TA_1 phonon mode is an intrinsic property of bulk Fe-based ordered Invar alloys,[5–11] the existence of this mode observed in our ordered $Fe_{0.75}Pt_{0.25}$ alloy NCs is a prerequisite for the existence of intrinsic Invar related properties of these NCs. Therefore, the observation of the [110] TA_1 mode provides strong indirect evidence for the persistence of Invar-related properties in Fe_3Pt NCs.

The remarkable reduction in the $g(E)$ intensity observed in the ~20 and ~25 meV (optical) phonon bands of the NCs [item (iii) above and Fig. 4(b)] may be due to one or more of the following reasons: (a) higher $L1_2$ ordering in the NCs than in the bulk ordered Fe_3Pt alloys of Refs. 10 and 11. Wiele *et al.*[9–11] have observed that, with increasing $L1_2$ ordering, the $g(E)$ contributions of these medium-energy bands decrease relative to that of the dominant ~30 meV peak,[50] and, moreover, that the ~30 meV peak shifts (by ~1 meV) to higher energy.[9–11] A similar blueshift is observed for our NCs [item (iv) above]. (b) In-plane projected $g(E)$; since our NRIXS experiment is performed at grazing incidence of the x-ray beam relative to the SiO_2/Si(111) wafer (substrate), it is the in-plane projected PDOS of our NCs that is measured. Any structural anisotropy, induced, for instance, by mechanical stress between NC and substrate, could result in changes in the PDOS, where certain phonon modes can be enhanced or suppressed relative to the isotropic case. Since Wiele *et al.*[9–11] used a polycrystalline bulk Fe_3Pt sample in their NRIXS experiment, their measured $g(E)$ is the isotropic case. (c) Phonon conversion at the NC interface; it is known that the presence of interfaces may change the character of optical phonons from pure longitudinal optical (LO) or transverse optical (TO) to a mixture involving LO, TO, and interface modes.[51] Since mixing results in larger dispersion, the PDOS in NCs can be modified.

It is worthwhile mentioning that $g(E)$ of our sample 2 (fcc $^{57}Fe_{0.75}Pt_{0.25}$) presents some resemblances with data previously measured by Tanaka *et al.*[52] on fcc-Fe precipitates (80 nm in diameter) using NRIXS. In particular, a dominant 31 meV peak (LA phonons), relatively strong TA bands near ~18 and ~23 meV, and a cutoff at ~37 meV was measured by Tanaka *et al.*,[52] but no feature near ~7–9 meV (typical for Fe-rich Fe-Pt alloys) was observed, contrary to the case of our fcc $^{57}Fe_{0.75}Pt_{0.25}$ NCs, Fig. 4(b) (inset).

We would like to emphasize that for our ordered $^{57}Fe_{0.75}Pt_{0.25}$ NCs [sample 2, Fig. 4(b)], we do not observe the low- and high-E enhancements of $g(E)$ that appear for the bcc $^{57}Fe_{0.8}Pt_{0.2}$ NCs in sample 1 [Fig. 4(a)]. As we discussed above, the low- and high-E enhancements of $g(E)$ is attributed to the specific core/shell structure of these NCs (bcc $^{57}Fe_{0.8}Pt_{0.2}$ core and PtSi shell). For sample 2, due to strong Pt surface segregation, a rather thick PtSi shell exists, (as indicated by our XPS data), preventing low- and high-E enhancements of $g(E)$, as expected.

Several important thermodynamic quantities can be derived from the measured PDOS,[32–36] such as the Lamb-Mössbauer (Debye-Waller) factor, kinetic energy, and the vibrational entropy and specific heat (all per atom). Table I displays the values obtained for the NCs in our samples 1–3, nanocrystalline Fe,[45] fcc Fe precipitates in Cu,[52] and bulk bcc Fe[53] for comparison. These quantities, together with the measured partial DOS, should allow a good test of the Fe-Fe, Fe-Pt, and Pt-Pt pair potentials in theoretical work. Generally, according to Table I and independent of the structure, all values given for the NCs are smaller than for bulk bcc Fe, except the kinetic energy per atom, which appears enhanced. The values for bcc $Fe_{0.8}Pt_{0.2}$ NCs are comparable to those of nanocrystalline Fe.

IV. SUMMARY

Summarizing, pronounced modifications (relative to the bulk) in the Fe-projected PDOS, $g(E)$, of isolated bcc $^{57}Fe_{0.8}Pt_{0.2}$ and fcc $^{57}Fe_{0.75}Pt_{0.25}$ (Invar type) NCs on a SiO_2/Si(111) support have been measured by NRIXS. Segregation of Pt atoms to the NC surface was observed by XPS upon annealing and Ar^+ sputter etching, leading to core/shell structures with Fe-rich cluster cores and PtSi cluster surfaces. The enhancement of the low- and high-E regions of $g(E)$ observed for the bcc NCs is in qualitative agreement with theoretical predictions. By contrast, due to their different shell structure, no such enhancement was observed for the fcc Fe NCs, which show characteristic phonon features of

bulk ordered Fe_3Pt Invar alloys. Our observation of the Invar-typical [110] TA_1 phonon mode in $^{57}Fe_{0.75}Pt_{0.25}$ NCs provides indirect evidence for the persistence of Invar-related effects in NCs. The obtained modified PDOS will affect the thermal stability and thermodynamic properties of the NCs relative to bulk materials. Moreover, our work demonstrates the power of NRIXS for the nondestructive metallurgical phase analysis of alloy nanoclusters.[54]

ACKNOWLEDGMENTS

Discussions with Ralf Meyer (Sudbury), M. Gruner, and P. Entel (Duisburg-Essen) are greatly appreciated. This work was supported by NSF (Grants No. CAREER-DMR-0448491 and No. DMR-0906562) and U.S. DOE (Grant No. DE-AC02-06CH11357).

*roldan@physics.ucf.edu

[1] B. Fultz, Prog. Mater. Sci. (to be published).
[2] N. A. Zarkevich, T. L. Tan, and D. D. Johnson, Phys. Rev. B **75**, 104203 (2007).
[3] For a review see E. F. Wassermann, in *Ferromagnetic Materials*, edited by K. H. Buschow and E. P. Wohlfarth (North-Holland, Amsterdam, 1990), Vol. VI, p. 240ff.
[4] D. D. Johnson and W. A. Shelton, in *The Invar Effect: A Centennial Symposium*, edited by J. Wittenauer (The TMS Society, Philadelphia, 1997), p. 63.
[5] K. Tajima, Y. Endoh, Y. Ishikawa, and W. G. Stirling, Phys. Rev. Lett. **37**, 519 (1976).
[6] Y. Noda and Y. Endoh, J. Phys. Soc. Jpn. **57**, 4225 (1988).
[7] J. Kästner, J. Neuhaus, E. F. Wassermann, W. Petry, B. Hennion, and H. Bach, Eur. Phys. J. B **11**, 75 (1999).
[8] J. Kästner, W. Petry, S. M. Shapiro, A. Zheludev, J. Neuhaus, Th. Roessel, E. F. Wassermann, and H. Bach, Eur. Phys. J. B **10**, 641 (1999).
[9] N. Wiele, H. Franz, and W. Petry, Physica B (Amsterdam) **263-264**, 716 (1999).
[10] N. Wiele, H. Franz, T. Ansthalten, and W. Petry, Annual Report from the Advanced Photon Source, Report No. ANL-0015, 1999.
[11] N. Wiele, Ph.D. dissertation, Technische Universität München, Munich, 2001.
[12] P. Entel, E. Hoffmann, P. Mohn, K. Schwarz, and V. L. Moruzzi, Phys. Rev. B **47**, 8706 (1993).
[13] M. Podgorny, Phys. Rev. B **43**, 11300 (1991).
[14] M. Podgorny, Phys. Rev. B **46**, 6293 (1992).
[15] W. A. Adeagbo, A. Zayak, and P. Entel, Phase Transitions **79**, 853 (2006).
[16] J.-H. Gao, Q.-F. Zhan, W. He, D.-L. Sun, and Z.-H. Cheng, Appl. Phys. Lett. **86**, 232506 (2005).
[17] J.-H. Gao, D.-L. Sun, Q.-F. Zhan, W. He, and Z.-H. Cheng, Phys. Rev. B **75**, 064421 (2007).
[18] A. M. Glezer, E. N. Blinova, V. A. Pozdnyakov, and A. V. Shelyakov, J. Nanopart. Res. **5**, 551 (2003).
[19] K. Kadau and P. Entel, Phase Transitions **75**, 59 (2002).
[20] K. Kadau, M. Gruner, P. Entel, and M. Kreth, Phase Transitions **76**, 355 (2003).
[21] L. Sandoval and H. M. Urbassek, Nano Lett. **9**, 2290 (2009).
[22] R. Meyer, L. J. Lewis, S. Prakash, and P. Entel, Phys. Rev. B **68**, 104303 (2003).
[23] A. Kara and T. Rahman, Surf. Sci. Rep. **56**, 159 (2005).
[24] H. Yildirim, A. Kara, S. Durukanoglu, and T. S. Rahman, Surf. Sci. **600**, 484 (2006).
[25] S. Durukanoglu, A. Kara, and T. S. Rahman, Phys. Rev. B **67**, 235405 (2003).
[26] S. R. Calvo and P. B. Balbuena, Surf. Sci. **581**, 213 (2005).
[27] H. Yildirim, A. Kara, and T. S. Rahman, J. Phys.: Condens. Matter **21**, 084220 (2009).
[28] B. Roldan Cuenya, A. Naitabdi, J. R. Croy, W. Sturhahn, J. Y. Zhao, E. E. Alp, R. Meyer, D. Sudfeld, E. Schuster, and W. Keune, Phys. Rev. B **76**, 195422 (2007).
[29] L. K. Ono, D. Sudfeld, and B. Roldan Cuenya, Surf. Sci. **600**, 5041 (2006).
[30] A. Naitabdi, L. K. Ono, F. Behafarid, and B. Roldan Cuenya, J. Phys. Chem. C **113**, 1433 (2009).
[31] J. R. Croy, S. Mostafa, L. Hickman, H. Heinrich, and B. Roldan Cuenya, Appl. Catal., A **350**, 207 (2008).
[32] M. Seto, Y. Yoda, S. Kikuta, X. W. Zhang, and M. Ando, Phys. Rev. Lett. **74**, 3828 (1995).
[33] W. Sturhahn, T. S. Toellner, E. E. Alp, X. Zhang, M. Ando, Y. Yoda, S. Kikuta, M. Seto, C. W. Kimball, and B. Dabrowski, Phys. Rev. Lett. **74**, 3832 (1995).
[34] A. I. Chumakov, R. Rüffer, H. Grünsteudel, H. F. Grünsteudel, G. Grübel, J. Metge, O. Leupold, and H. A. Goodwin, Europhys. Lett. **30**, 427 (1995).
[35] A. I. Chumakov and W. Sturhahn, Hyperfine Interact. **123-124**, 781 (1999).
[36] W. Sturhahn, Hyperfine Interact. **125**, 149 (2000).
[37] L. Zwell, G. R. Speich, and W. C. Leslie, Metall. Trans. **4**, 1990 (1973).
[38] W. B. Pearson, *Handbook of Lattice Spacings and Structures of Metal Alloys* (Pergamon, Oxford, 1967), Vol. 2, p. 821.
[39] NIST X-ray Photoelectron Spectroscopy Database, Version 3.4 (Web Version) http://srdata.nist.gov/xps/index.htm
[40] A. Ethirajan, U. Wiedwald, H.-G. Boyen, B. Kern, L. Han, A. Klimmer, F. Weigl, G. Kästle, P. Ziemann, K. Fauth, J. Cai, R. J. Behm, A. Romanyuk, P. Oelhafen, P. Walther, J. Biskupek, and U. Kaiser, Adv. Mater. (Weinheim, Ger.) **19**, 406 (2007).
[41] P. J. Grunthaner, F. J. Grunthaner, and A. Madhukar, J. Vac. Sci. Technol. **20**, 680 (1982).
[42] C. Creemers and P. Deurinck, Surf. Interface Anal. **25**, 177 (1997).
[43] U. B. Demirci, J. Power Sources **173**, 11 (2007).
[44] Y. Ma and P. B. Balbuena, Surf. Sci. **602**, 107 (2008).
[45] B. Fultz, C. C. Ahn, E. E. Alp, W. Sturhahn, and T. S. Toellner, Phys. Rev. Lett. **79**, 937 (1997).
[46] B. Roldan Cuenya, W. Keune, R. Peters, E. Schuster, B. Sahoo, U. von Hörsten, W. Sturhahn, J. Zhao, T. S. Toellner, E. E. Alp, and S. D. Bader, Phys. Rev. B **77**, 165410 (2008).
[47] R. Meyer, S. Prakash, and P. Entel, Phase Transitions **75**, 51 (2002).

[48] The high-energy oscillations above ~40 meV in Fig. 4(b) are believed to be an artifact due to the low count rate in that energy regime and the slightly higher background count rate for $E > \sim 40$ meV as compared to $E < \sim -40$ meV in Fig. 3(b), combined with the mathematical Fourier-log procedure employed in the PHOENIX software used for data evaluation (Ref. 36).

[49] B. Fultz, T. A. Stephens, E. E. Alp, M. Y. Hu, J. P. Sutter, T. S. Toellner, and W. Sturhahn, Phys. Rev. B **61**, 14517 (2000).

[50] In a recent molecular-dynamics simulation of the PDOS of $Cu_{3-x}Au_x$ alloy NCs, a suppression of the low-E phonon bands relative to the high-E peak height and a blueshift of the high-E peak with increasing $L1_2$ ordering was predicted by R. Meyer, Laurentian University, Sudbury, Canada (private communication).

[51] B. Jusserand and M. Cardona, in *Light Scattering in Solids V*, Topics in Applied Physics, edited by M. Cardona and G. Güntherodt (Springer, Heidelberg, 1989), Vol. 66, p. 49.

[52] T. Tanaka, A. Tajima, R. Moriizumi, C. Oshima, Y. Tsunoda, M. Seto, S. Kitao, and T. Mitsui, J. Phys. Soc. Jpn. **74**, 1762 (2005).

[53] G. Shen, W. Sturhahn, E. E. Alp, J. Zhao, T. S. Toellner, V. B. Prakapenka, Y. Meng, and H.-R. Mao, Phys. Chem. Miner. **31**, 353 (2004).

[54] B. Roldan Cuenya, L. K. Ono, J. R. Croy, A. Naitabdi, H. Heinrich, J. Zhao, E. E. Alp, W. Sturhahn, and W. Keune, Appl. Phys. Lett. (to be published).